

# Removal of Fluoride from Drinking Water Using Novel Adsorbent Magnesia-Hydroxyapatite

Poonam Mondal · Suja George

Received: 19 March 2015 / Accepted: 22 June 2015 / Published online: 7 July 2015  
© Springer International Publishing Switzerland 2015

**Abstract** In many parts of the world, fluoride in drinking water is responsible for notable public health issues. The present study is aimed to prepare a new adsorbent magnesia-hydroxyapatite (Mg-HAP) that can serve as a valuable defluoridating agent. Characterization of the synthesized adsorbent was done by Fourier transform infrared spectroscopy (FTIR), X-ray diffraction (XRD), Transmission electron microscope (TEM), and Scanning electron microscope (SEM)/Energy-dispersive X-ray spectroscopy (EDX) analysis to reveal the bonding patterns, phase characteristics, and microstructural and morphological details. The influences of pH, adsorbent dose, contact time, and initial fluoride concentration and the effect of interfering anions were studied. The defluoridation capacity was evaluated to be 1.4 mg/g, and the adsorbent showed very good capability to remove fluoride from contaminated water over a wide range of pH. Equilibrium modeling was done, and the experimental data was fitted into Langmuir, Freundlich, Temkin, and Dubinin-Radushkevich isotherms. Study of the kinetic data for the adsorption process revealed that it follows pseudo-second-order reaction. It also indicated that the intraparticle diffusion contributes to the rate-determining step in the process. The quality of treated water was analyzed for total dissolved solids (TDS), turbidity, residual calcium, residual phosphorus content, electrical conductivity, hardness, and total alkalinity. The results obtained were very

promising and confirmed the prospects of usage of Mg-HAP in defluoridation of drinking water.

**Keywords** Magnesia-hydroxyapatite · Defluoridation · Fluoride · Adsorbent

## Abbreviations

- $q_e$  Amount of adsorption at equilibrium (mg/g)  
 $q_t$  Amount of adsorption at time  $t$  (mg/g)  
 $C_0$  Initial concentrations of fluoride (mg/L)  
 $C_e$  Equilibrium concentrations of fluoride (mg/L)  
 $C_t$  Concentration of fluoride at time  $t$  (mg/L)  
 $v$  Volume of the aqueous solution (L)  
 $m$  Adsorbent mass (g)  
 $Q_0$  Maximum adsorption capacity reflecting complete monolayer (mg/g)  
 $R_L$  Separation factor depicting favorability of the process  
 $b$  Langmuir constant related to energy  
 $K_f$  Freundlich constants (mg/g)  
 $N$  Heterogeneity factor  
 $R$  Universal gas constant (8.314 J/mol K)  
 $T$  Temperature (K)  
 $A_T$  Temkin isotherm equilibrium binding constant (L/g)  
 $B_T$  Temkin isotherm constant  
 $b_1$  Adsorption rate constant of first order reaction ( $\text{min}^{-1}$ )  
 $b_2$  Adsorption rate constant of first order reaction ( $\text{g mg}^{-1} \text{min}^{-1}$ )  
 $k_i$  Intraparticle diffusion rate constant ( $\text{mg g}^{-1} \text{min}^{-1/2}$ )  
 $a$  Initial adsorption rate ( $\text{mg g}^{-1} \text{min}^{-1}$ )  
 $\alpha$  Desorption rate ( $\text{g mg}^{-1}$ )

P. Mondal (✉) · S. George  
Department of Chemical Engineering, Malaviya National  
Institute of Technology, Jaipur, Rajasthan 302017, India  
e-mail: poonam.mbiotech@gmail.com

$B$	Dubinin-Radushkevich isotherm constant
$q_d$	Theoretical isotherm saturation capacity (mg/g)
$\varepsilon$	Polanyi potential
$k_p$	Particle diffusion coefficient ( $\text{min}^{-1}$ )

## 1 Introduction

Availability of safe water for consumption is the one of the most important gifts to mankind. But, unfortunately, the increase in concentration of contaminants such as fluoride above the permissible limit in groundwater resources over the years has become a serious matter of concern in many countries such as China, India, Pakistan, Turkey, Iraq, Afghanistan, Mexico, and Thailand (Gogoi et al. 2015; Ayoob and Gupta 2006; Maheshwari 2006). Elevated levels of fluoride in groundwater are a result of dissolution of minerals like fluorite, apatite, and topaz from the local bedrock (Murray 1986). Fluoride is such an element which needs to maintain a balance in the environment so that it just acts as a beneficial additive and not a detrimental contaminant. The permissible limit of fluoride ion concentration in drinking water is 1.5 mg/L (WHO 2011). Some of the hazardous effects due to consumption of fluoride in human body are illustrated in Fig. 1.

Many fluoride remediation techniques and treatments such as adsorption (Mondal and George 2014), nano-filtration (Hu and Dickson 2006), reverse osmosis (Sehn 2007), and electro-coagulation (Essadki et al. 2009) are focused for solving the complicated health issues raised due to excessive fluoride in potable water. However, as reported in literature, adsorption technology is the most preferred method of defluoridation for impoverished people and mostly living in developing countries (Fawell et al. 2006). Adsorption process is a simple but attractive technique because of its removal

efficiency, selectivity, high-quality effluent, as well as its cost-effectiveness (Fan et al. 2003; Liu et al. 2010).

Most widely used adsorbents for defluoridation are compounds or materials inhering aluminum, calcium, and magnesium. Aluminum is neurotoxic in nature, and residual aluminum in drinking water has been reported by researchers (George et al. 2010). Keeping this fact in mind, affinity of calcium and magnesium ions towards fluoride has been explored in form of adsorbents. Calcium-based adsorbents such as calcite, limestone, and hydroxyapatite are found to be potential defluoridating agents (Mondal et al. 2014; Jain and Jayaram 2009; Jimenez-Reyes and Solache-Rios 2010). Hydroxyapatite (HAP) is a calcium phosphate-based bioceramic, having the chemical formula  $\text{Ca}_5(\text{PO}_4)_3(\text{OH})$  with the Ca/P ratio being 1.67 and is being used in the medical field widely (Chen et al. 2004; Mehta et al. 2014). The HAP structure can be represented as two subsystems: first, the calcium channels in which the  $-\text{OH}$  groups are arranged and second the main framework of calcium phosphate. Fluoride ions can be substituted in place of hydroxide ions in the hydroxyapatite structure to form fluorapatite which is more thermodynamically stable than HAP itself (Orlovskii et al. 2002). Sorption behavior of hydroxyapatite for removing fluoride from water has been studied by observing the effect of pH and contact time (Jimenez-Reyes and Solache-Rios 2010; He and Cao 1996). Nano-hydroxyapatite has been studied by some researchers and used for evaluating its capacity for fluoride removal (Sundaram et al. 2008; Sundaram et al. 2009; Gao et al. 2009). However, no reports have been found in the literature regarding defluoridation using magnesia-hydroxyapatite; therefore, in this study, this novel adsorbent was explored for its fluoride removal capabilities. Magnesium ions also have a high affinity towards fluoride, and magnesium compounds are well known to show high defluoridation capacity

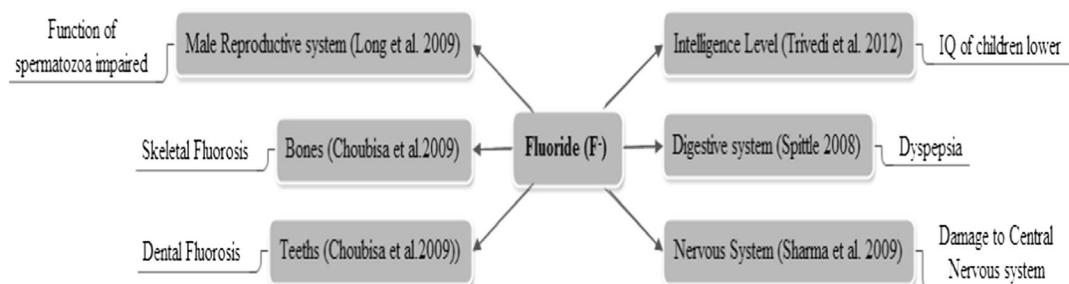


**Fig. 1** Effects of excess fluoride in human body

such as magnesia-amended activated alumina (Maliyekkal et al. 2008). Magnesium influences both matrix and mineral metabolism in human body, and depletion in magnesium levels affects all stages of skeletal metabolism adversely (Percival 1999).

To increase the defluoridation capacity of hydroxyapatite, an attempt has been made to amend magnesia with the bioceramic hydroxyapatite to form magnesia-hydroxyapatite (Mg-HAP). The present study investigates the feasibility of the Mg-HAP powder for fluoride removal from aqueous solution. The main objectives were (i) to evaluate the effect of adsorbent concentration, contact time, pH, and coexisting anions on the fluoride removal capacity of Mg-HAP and (ii) describe adsorption equilibrium using different adsorption isotherms (iii) to understand the fluoride adsorption kinetics.

## 2 Materials and Methods

### 2.1 Chemicals and Reagents

For preparation of magnesia-hydroxyapatite, hydroxyapatite was received from Clarion Pharmaceuticals Ltd., New Delhi, India, and its chemical composition is given in Table 1. All chemicals used in the present study were of analytical reagent grade and were obtained from E-Merck India Ltd, Mumbai, India. A stock solution of fluoride was prepared by dissolving 2.21 g of sodium fluoride in 1 L of double distilled water, and working solution of 10 mg/L was obtained by appropriate dilution from the stock solution. Total ionic strength adjustment buffer (TISAB) was prepared by availing 58 g of sodium chloride, 4 g CDTA, and 57 mL of glacial acetic acid. For adjusting the pH of the buffer to 5.0 to 5.5, 5 M NaOH solution is used. Double distilled water was used for all purposes in this study to avoid any issue related to ionic contamination.

**Table 1** Chemical composition of hydroxyapatite

Composition	Percentage present
Calcium	22.80
Phosphorus	10.15
Moisture	1.96
Ash content	61.58
Other	3.51

### 2.2 Preparation of Mg-HAP Adsorbent

The adsorbent Mg-HAP was prepared using powdered magnesium hydroxide  $[\text{Mg}(\text{OH})_2]$  and HAP. These powders were sieved separately to 200–250 British Standard Sieve (BSS) mesh size and mixed in 1:1 ratio. The product thus obtained was kept in a muffle furnace for calcination at 800 °C for 180 min. It was then sieved to 200–250 BSS mesh size again for getting uniform particle size, and the material (Mg-HAP) thus obtained was used for the fluoride mitigation from drinking water. Batch fluoride adsorption experiments were conducted to study and optimize various operational parameters such as adsorbent dose, contact time, pH, effect of co-ions, and initial fluoride concentration.

### 2.3 Characterization of Mg-HAP

The bonding patterns and functional groups in the prepared Mg-HAP were characterized using a PerkinElmer Fourier transform infrared spectrophotometer (FTIR) (UTR TWO) in the range of 450–4,000  $\text{cm}^{-1}$  with a resolution of 4  $\text{cm}^{-1}$ . The adsorbent was mixed with KBr in the ratio of 1:50 in order to remove the scattering effects due to large crystals. Thereafter, a translucent pellet was obtained by using a KBr press (model M-15, Technosearch Instruments), and the pellet was placed in a spectrometer. Then, the graphic representation of the spectra was taken. X-ray diffraction patterns were recorded on PANanalytical X'pert powder X-ray diffractometer for structural identification of prepared Mg-HAP. The samples were scanned for  $2\theta$  range from 10° to 80° with step size of 0.15° and scan step time of 3 s.

The crystallographic structure of Mg-HAP was determined with transmission electron microscope (Technai G2T20). For transmission electron microscope (TEM) analysis, samples were prepared by ultrasonic vibration method. A small amount of sample was suspended in ethanol solution and subjected to ultrasonic vibrations in an ultrasonic cleaner (Buehler Ultramet) for 30 min for dispersion of the powder homogeneously. Simultaneously, for analyzing the elemental compositions of the sample, energy-dispersive spectroscopy (EDS) was employed (Xflash 6TI30 Bruker). The surface morphology and microstructure of Mg-HAP were visualized by means of scanning electron microscopy (Nova Nano SEM 450). All the samples were coated with thin film of platinum using JEOL/JFC1600 Auto

fine coater to reduce charging of the sample so that conductivity of sample can be increased. The experiment is performed at an accelerating voltage of 18 kV.

## 2.4 Batch Fluoride Adsorption Studies

Batch studies were conducted using 100 mL of fluoride solution in PVC containers. A known weight of Mg-HAP adsorbent was added and kept for shaking in an orbital shaker (model no. CIS-24BL, Remi Instruments Mumbai, India) in order to attain the adsorption equilibrium. Studies were carried out varying shaking speeds for determining the optimum speed for point of maximum adsorption. All adsorption experiments were performed out at room temperature ( $25 \pm 0.5$  °C).

The specific amount of fluoride adsorbed was calculated using following expression:

$$q_e = (C_i - C_e) \times \frac{V}{m}$$

## 2.5 Sample Analysis

After performing fluoride adsorption equilibrium experiments, the samples were filtered using Whatman filter paper no. 42 and analyzed for residual fluoride concentration using ion selective electrode (Orion Versa Star 93). Ion meter calibrations were done using fluoride standards prepared from the stock solutions. For de-complexation of complexes and avoiding interference with the electrode performance, an ionic strength fixer and buffer TISAB-II solution were added in 1:1 proportion to 10-mL sample solution. Calibrations were also checked in between sample measurements to ensure the accuracy of readings obtained. The same ion meter coupled with pH electrode (Orion ROSS combination pH electrode) was used to measure the pH of the solution. Leaching of calcium from Mg-HAP adsorbent was studied using the ion meter coupled with calcium electrode. The same experimental procedure was followed to study the effect of the adsorbent dose, contact time, pH, initial fluoride concentration, and coexisting ions on adsorption of fluoride on Mg-HAP powder. Total dissolved solids (TDS) and electrical conductivity analysis of treated water was performed using conductivity electrode of ion meter, while turbidity present in the aqueous solution was measured with a turbidity meter (NT4000, Spectra Lab). The total hardness, total alkalinity, and

phosphorus concentration of solution were calculated by APHA standard procedures (APHA 1995).

## 3 Results and Discussion

### 3.1 Characterization Studies

The synthesized Mg-HAP was characterized for evaluating the functional groups, bonding patterns, crystallinity, structure, and surface morphology, and the obtained results are as follows:

#### 3.1.1 FTIR

The FTIR was performed on Mg-HAP to evaluate the functional groups and bonding pattern. The spectrum is presented in Fig. 2. The peak observed around  $3,571.43$   $\text{cm}^{-1}$  confirmed the presence of  $-\text{OH}$  bond (Russell et al. 1996). This peak is mainly due to  $\text{O}-\text{H}$  stretching vibration in HAP. The peak obtained at  $1,043.24$   $\text{cm}^{-1}$  is associated with the stretching modes of the  $\text{P}-\text{O}$  bonds of HAP (Sargin et al. 1997). The double peak at  $602.17$  and  $567.5$   $\text{cm}^{-1}$  is due to bending modes of  $\text{P}-\text{O}$  bonds in phosphate groups (Raman and Venkatesh 2004). The asymmetric  $\text{P}-\text{O}$  vibration of  $\text{PO}_4^{3-}$  observed at  $961.78$   $\text{cm}^{-1}$  is distinguishable which also represents bending vibration of  $\text{PO}_4^{3-}$  in hydroxyapatite. Hydroxyapatite synthesis requires an alkaline condition that is maintained using ammonium solution. Although repeated washing was done with double distilled water, still there is a possibility of small amount of ammonium ions in the hydroxyapatite. The FTIR spectra displayed a small broad peak at  $1,422.6$   $\text{cm}^{-1}$ , which is characteristic peak of  $\text{NH}_4^+$  group.

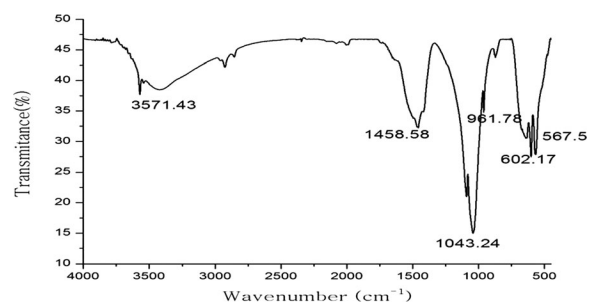


**Fig. 2** FTIR spectrum of Mg-HAP

### 3.1.2 XRD

According to the results obtained by XRD analysis, Mg-HAP exhibited crystalline structure as shown in Fig. 3, and all the peaks matched the standard JCPDS pattern (hydroxyapatite 00-024-0033, MgO 00-045-0946). Peaks of magnesium oxide (MgO) are obtained in the diffraction pattern due to the calcination of magnesium hydroxide present in Mg-HAP.

### 3.1.3 TEM/EDX

TEM micrograph of Mg-HAP at different magnifications is shown in Fig. 4. From TEM studies, it was found that the average size of particles was 70–150 nm in length and 30–40 nm in width. The microstructures exhibit elongated morphology; however, it appears agglomerated at places and the crystals are arranged in different orientations. The crystalline nature of the Mg-HAP adsorbent was confirmed through dark field image of TEM. The energy-dispersive X-ray spectroscopy (EDX) spectrum of Mg-HAP given in Fig. 4 depicts the presence of magnesium, calcium, phosphorus, and oxygen in the structure. No impurities were observed in the spectrum; hence, pure Mg-HAP was obtained. A peak for copper was obtained, since the grid used for mounting the sample is made of copper. The mean crystallite size was also calculated from Scherer formula, and it showed that the nanocrystals have an average size of 65 nm which is close to the particle size observed in TEM (70 nm approximately).

### 3.1.4 SEM

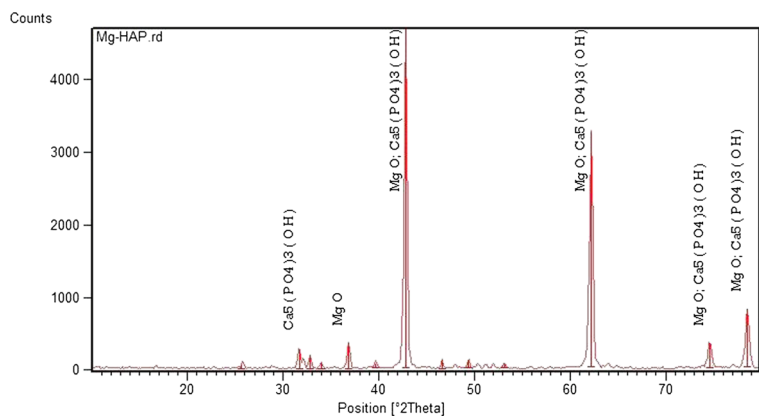
The SEM image of prepared Mg-HAP is shown in Fig. 5. Numerous dense agglomerations of particles are observed in the SEM image. Elemental mapping images for calcium, phosphorous, and magnesium are also shown in Fig. 6, which provides an overview of location of different elements present according to the color assigned, viz. red for phosphorous, blue for magnesium, and green for calcium.

## 3.2 Batch Fluoride Adsorption Studies on Mg-HAP

### 3.2.1 Effect of Adsorbent Dose

The experimental studies revealed that an optimum shaking speed of 200 rpm is required for attaining 92.34 % of fluoride removal using 10 g/L of Mg-HAP for initial fluoride concentration of 10 mg/L at pH  $7.5 \pm 0.1$  and  $25 \pm 0.5$  °C for a contact time of 180 min as shown in Fig. 7. The effect of adsorbent dose on removal of fluoride using Mg-HAP is shown in Fig. 8. It was observed that percentage removal of fluoride increased with the increase in adsorbent dose gradually; however, beyond 10 g/L of adsorbent dosage, no significant removal was observed. The amount of fluoride loaded per unit weight of adsorbent gradually decreased for the same due to lower concentration of fluoride available at higher adsorbent dose. It was observed that percent fluoride removal increased from 48.7 to 92.34 % with an increase in Mg-HAP dose from 2 to 10 g/L at an initial fluoride concentration of 10 mg/L. This is due to the increase in the ratio of active sites to fluoride ions

**Fig. 3** XRD patterns of Mg-HAP



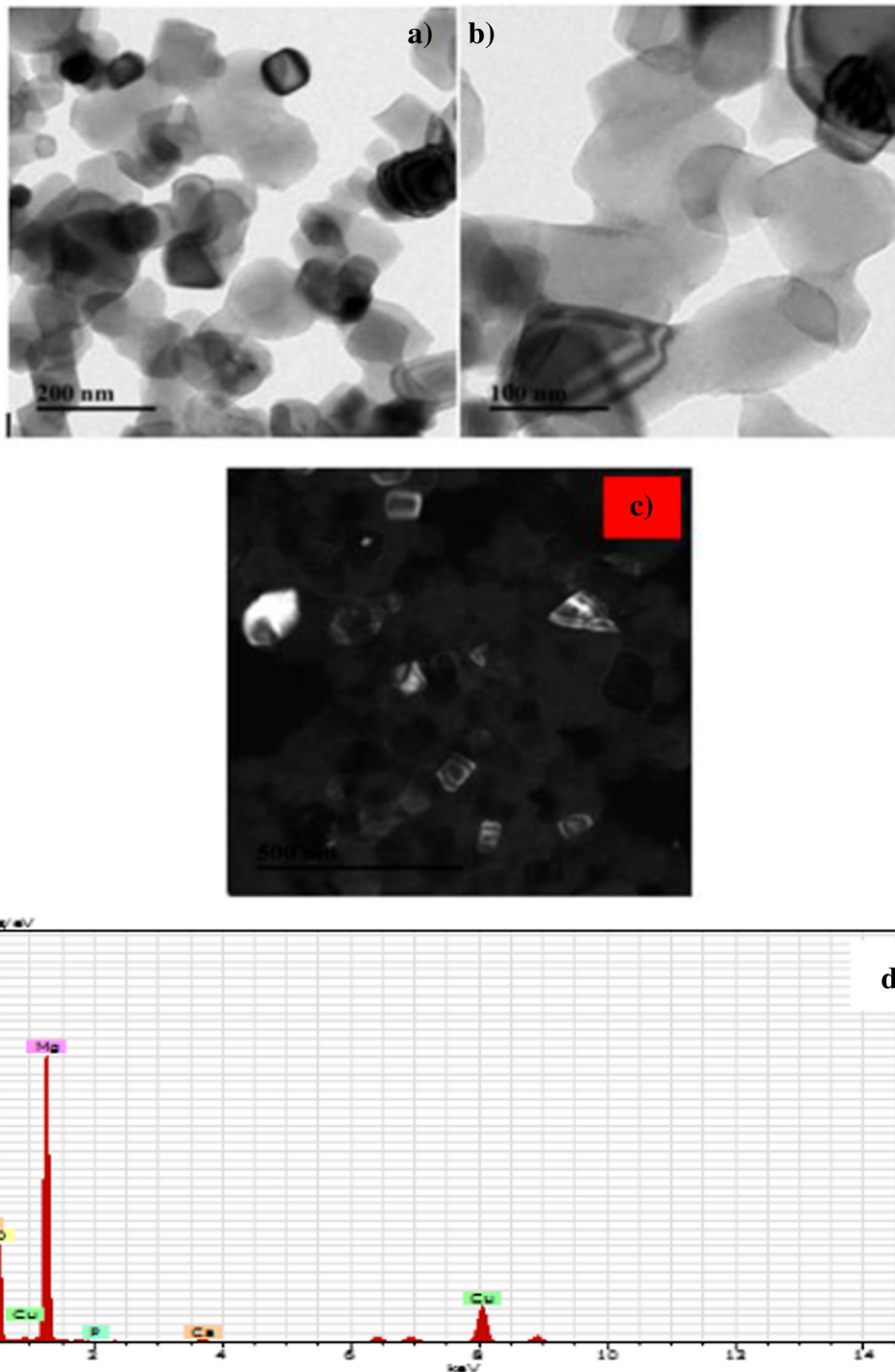


**Fig. 4** a TEM image at 200 nm. b TEM image at 100 nm. c Dark field image showing crystalline nature of Mg-HAP. d EDX spectra of Mg-HAP

present. On further increasing the dose of adsorbent to 24 g/L, no significant removal was observed because of the very low equilibrium concentration of fluoride, in

other words low driving force was responsible for adsorption. The fluoride concentration was reduced from 10 to 0.766 mg/L in aqueous solution thus attaining the

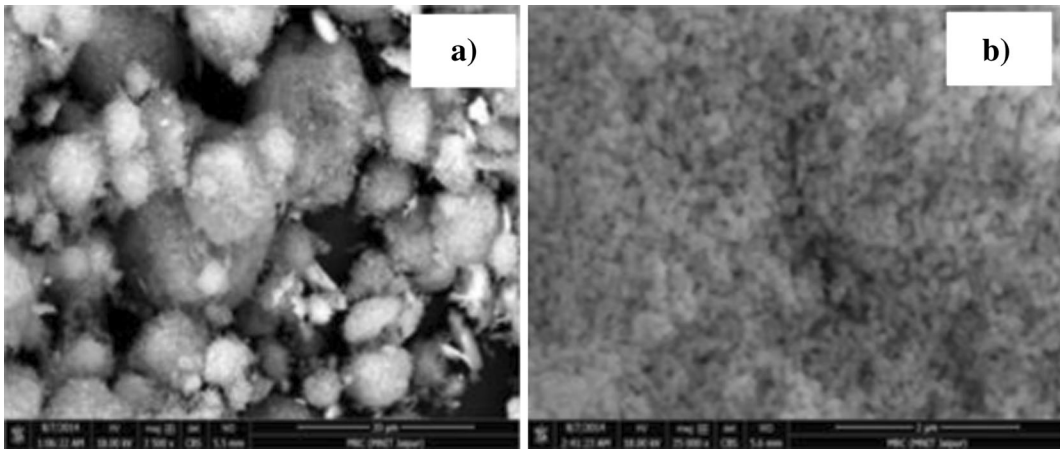


Fig. 5 SEM image of Mg-HAP at magnifications of **a**  $\times 3,500$  and **b**  $\times 35,000$

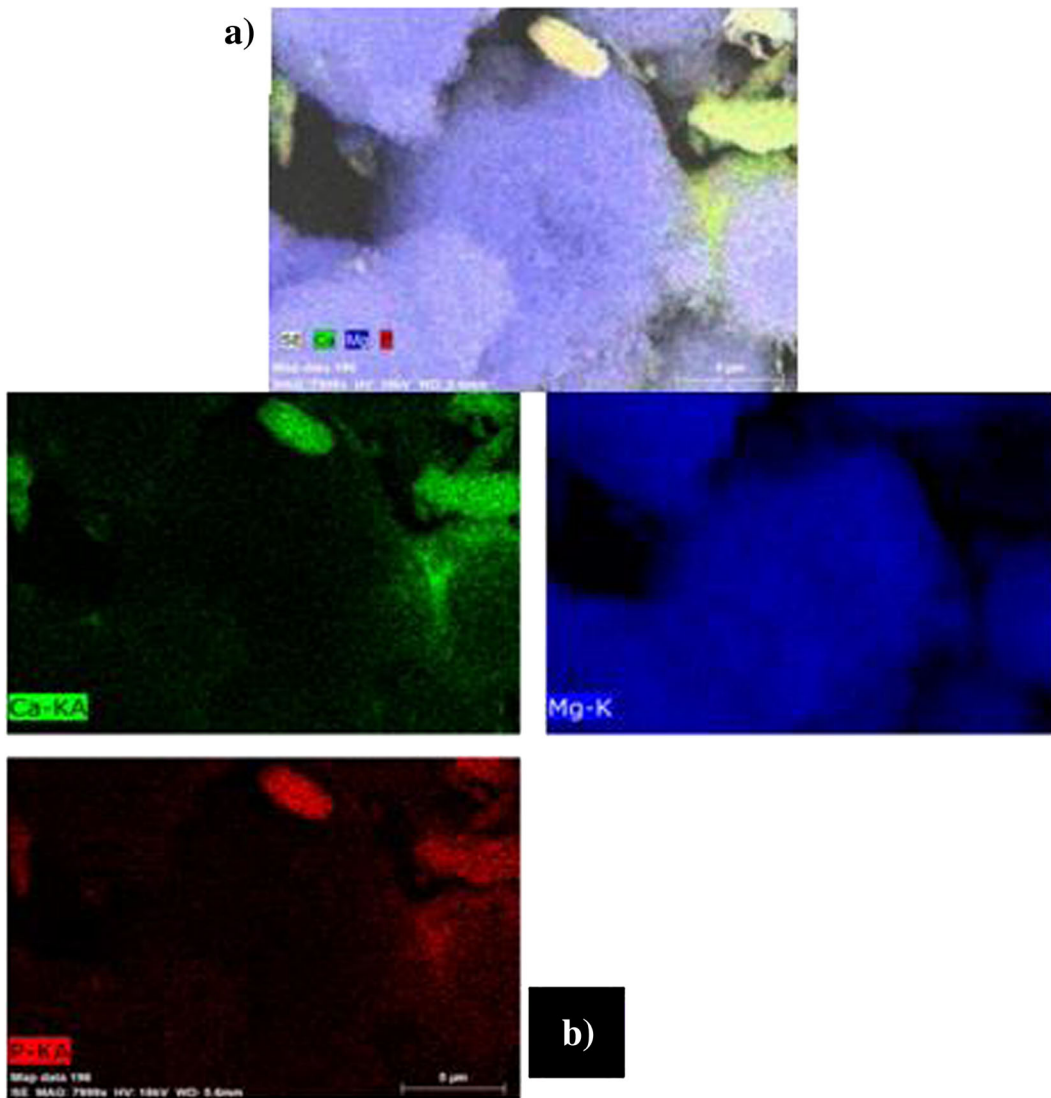


Fig. 6 Mapping of elements. **a** Mg-HAP adsorbent. **b** Individual element distribution of Ca, Mg, and P

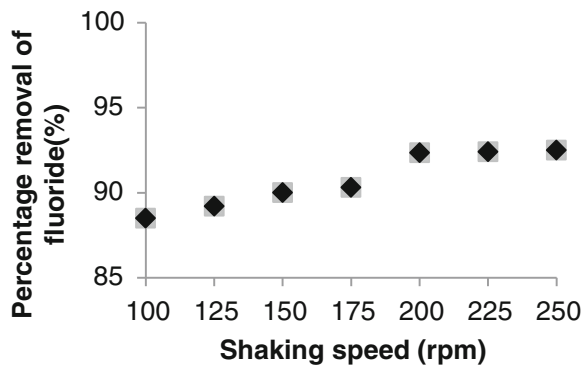


Fig. 7 Optimization of shaking speed for defluoridation studies

permissible limit of fluoride in drinking water according to WHO (1.5 mg/L) and Indian Standard Drinking water specification (1.0 mg/L) at an Mg-HAP dose of 10 g/L. Hence, 10 g/L dose was considered for further studies.

### 3.2.2 Effect of Contact Time

The percentage removal of fluoride as a function of contact time for Mg-HAP is shown in Fig. 9. It was observed that a fluoride removal of 92.54 % occurred in 180 min with a fixed amount of Mg-HAP (10 g/L). As the contact time between adsorbate and adsorbent increases, it is noticed that the percentage of fluoride removal also increases up to equilibrium point (180 min) and then becomes constant and no significant removal occurs.

### 3.2.3 Effect of pH

The pH of the aqueous solution plays an important role in controlling the fluoride adsorption at the adsorbent–water interface. Therefore, the adsorption of fluoride on

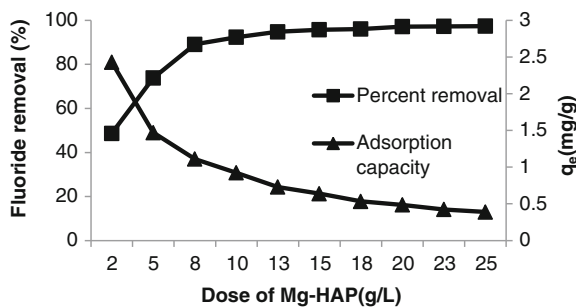


Fig. 8 Effect of dosage ( $F^-$  concentration 10 mg/L, dose 2 to 24 g/L, pH 7.5±0.1, agitation time 3 h, agitation rate 200 rpm, temperature 25±0.5 °C)

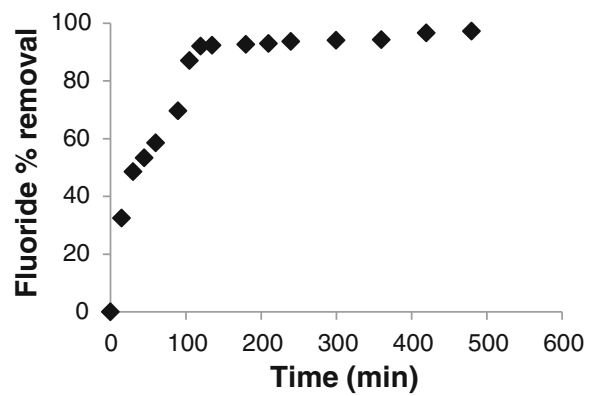


Fig. 9 Effect of contact time ( $F^-$  concentration 10 mg/L, pH 7.5±0.1, agitation time 15 to 480 min, agitation rate 200 rpm, Mg-HAP dose, 10 g/L, temperature 25±0.5 °C)

Mg-Hap was examined at various pH ranges from pH 3 to 10 with 10 mg/L as initial fluoride concentration at room temperature (25±0.5 °C). The pH of the working solution was controlled by adding sufficient 0.1 N HCl/NaOH solutions. It can be inferred from Fig. 10 that fluoride removal was approximately constant over the entire pH range of 3 to 10 for Mg-HAP. Therefore, the present adsorption process is not pH-dependent as compared to conventionally used adsorbents such as activated alumina which is an added advantage of the Mg-HAP over other adsorbents. As drinking water pH should be within 6.5 to 8.5, Mg-HAP exhibits no variation in fluoride adsorption capacity in this pH range. Concentration of dissolved calcium ions at different pH varying from 3 to 10 is also given in Fig. 11. It was observed that at pH 9 and 10 (alkaline conditions), there is some release of calcium into water of 17.4 and 19.13 mg/L, respectively. Leaching of

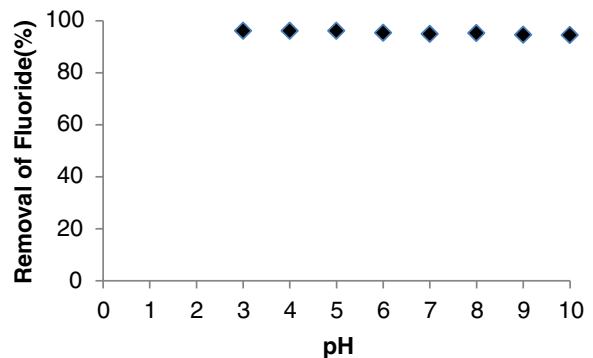
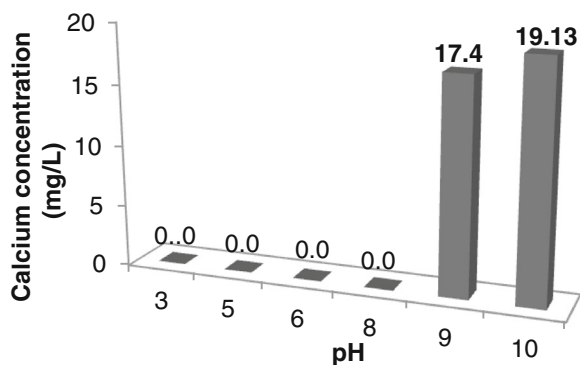


Fig. 10 Effect of pH ( $F^-$  concentration 10 mg/L, pH 3 to 10, Mg-HAP dose 10 g/L, agitation time 3 h, agitation rate 200 rpm, temperature 25±0.5 °C)





**Fig. 11** Calcium leaching from treated water ( $F^-$  concentration 10 mg/L, pH 3 to 10, Mg-HAP dose 10 g/L, agitation time 3 h, agitation rate 200 rpm, temperature  $25 \pm 0.5$  °C)

calcium in alkaline conditions has also been reported while working with calcium aluminate adsorbent (Sakhare et al. 2012).

### 3.2.4 Effect of the Presence of Coexisting Ions

Drinking water usually contains other ions such as chloride, sulfate, nitrate, phosphate, and bicarbonate, which may compete with fluoride during the adsorption process. Hence, it is necessary to study the effect of coexisting ions on the removal of fluoride. The most common ions found in groundwater are chloride, sulfate, and bicarbonate (Ravindra and Garg 2007; Tatawat and Chandel 2008). Some other prominent ions are phosphate and nitrate. Batch adsorption studies were performed at varying initial concentrations of  $Cl^-$ ,  $SO_4^{2-}$ ,  $NO_3^{2-}$ ,  $PO_4^{2-}$ , and  $HCO_3^-$  in the range of 100, 200, and 300 mg/L by keeping other parameters such as Mg-HAP dosage (10 g/L), fluoride concentration (10 mg/L), temperature ( $25 \pm 0.5$  °C), shaking speed (200 rpm), and contact time (180 min) constant.

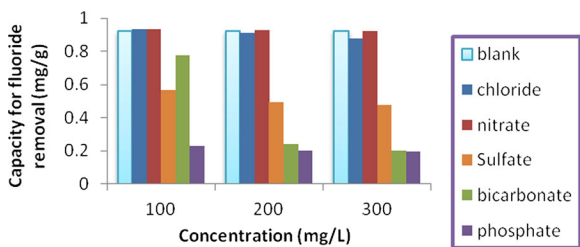


**Fig. 12** Effect of presence of other ions on removal capacity of fluoride ( $F^-$  concentration 10 mg/L, pH  $7.5 \pm 0.1$ , agitation time 3 h, agitation rate 200 rpm, Mg-HAP dose 10 g/L, temperature  $25 \pm 0.5$  °C)

The effect of co-ions on the fluoride removal efficiency for Mg-HAP is depicted in Fig. 12. It was observed that even in the presence of high concentrations of nitrate and chloride ions (300 mg/L), there were negligible effect on fluoride removal capacity. This is due to the fact that fluoride ions competed more than chloride and nitrate ions. However, the presence of phosphate ions in aqueous medium exhibited strong hindrance in fluoride adsorption capacity. The orders of interference by these competing ions from lower to higher are in the following order: nitrate < chloride < sulfate < bicarbonate < phosphate, but such high concentrations of ions are seldom present in drinking water.

### 3.2.5 Effect of Initial Fluoride Concentration

The effect of initial fluoride concentration on fluoride adsorption by Mg-HAP was studied by keeping all other parameters constant (Mg-HAP dose 10 g/L, temperature  $25 \pm 0.5$  °C, shaking speed 200 rpm, contact time 180 min, and pH  $7.5 \pm 0.1$ ) as shown in Fig. 13. It was observed that with an increase in fluoride concentration, residual fluoride in treated water also increases due to more availability of fluoride ions at higher fluoride concentration for adsorption. Eventually, the binding capacity of the adsorbent reaches saturation, resulting in an increase of residual fluoride in water.

## 4 Adsorption Equilibrium

Adsorption of fluoride onto Mg-HAP involves the establishment of equilibrium between the fluoride adsorbed on the surface of Mg-HAP and the concentration of fluoride

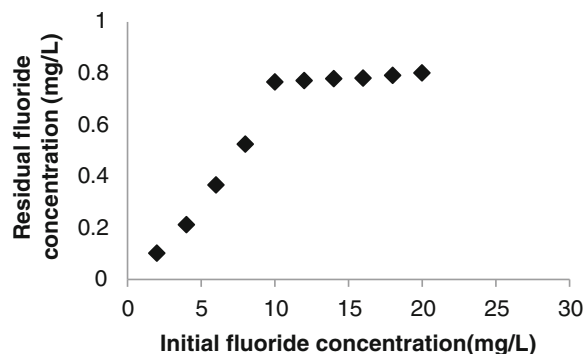


**Fig. 13** Effect of initial fluoride concentration ( $F^-$  concentration 2 to 20 ppm, pH  $7.5 \pm 0.1$ , agitation time 180 min, agitation rate 200 rpm, Mg-HAP dose 10 g/L, temperature  $25 \pm 0.5$  °C)

**Table 2** Values of different parameters of Langmuir, Freundlich, Temkin and Dubinin-Radushkevich isotherm

Isotherms	Equation	Parameters	Value
Langmuir	$\frac{C_e}{q_e} = \frac{1}{bQ_0} + \frac{C_e}{Q_0}$	$b$ (L/g)	3.909
		$Q_0$ (mg/g)	1.400
		$R_L$	0.102
		$K_{ap}$	5.472
		$R^2$	0.989
		$\chi^2$	0.025
Freundlich	$\log q_e = \log K_f + \frac{1}{n} \log C_e$	$1/n$	0.835
		$K_f$ (mg/g)	1.280
		$R^2$	0.986
		$\chi^2$	0.064
Temkin	$q_e = B_T \ln A_T + B_T \ln C_e$	$A_T$ (L/mg)	6.619
		$B_T$	0.470
		$R^2$	0.976
		$\chi^2$	1.31
Dubinin-Radushkevich	$\ln q_e = \ln q_d - B \varepsilon^2$ Where, $\varepsilon = RT \ln \left[ 1 + \frac{1}{C_e} \right]$	$q_d$ (mg/g)	1.024
		$B$	5E-8
		$R^2$	0.987
		$\chi^2$	0.19

ions in solution. The variation of extent of adsorption with concentration of solute is represented by adsorption isotherms. The isotherm provides an idea about effectiveness of Mg-HAP in removing fluoride ion from water, also it indicates the maximum amount of fluoride adsorbed by the prepared Mg-HAP. Four isotherms were used to model the adsorption mechanism. The expressions and values for parameters of Langmuir, Freundlich, Temkin, and Dubinin-Radushkevich isotherm are presented in Table 2. The Langmuir isotherm states a monolayer type of adsorption, and molecules of adsorbate do not deposit on each other. Langmuir isotherm is also evaluated by a separation factor  $R_L$ , which determines the feasibility of the isotherm:

$$R_L = 1 / (1 + K_a C_0)$$

Freundlich isotherm predicts a multilayer form of adsorption and provides detailed idea about effectiveness of the adsorbent and maximum amount of adsorbate that will get adsorbed by adsorbent. Freundlich isotherm was plotted with  $\log q_e$  versus  $\log C_e$ . A smaller value of  $1/n$  depicts a better adsorption mechanism and formation of relatively stronger bond between adsorbate and adsorbent.

The Temkin isotherm contains a factor ( $A_T$ ) that explicitly considers adsorbate-adsorbent interactions. By

ignoring the extremely low and high value of concentration, it assumes that the heat of adsorbents of all molecules in the layer would decrease linearly rather than logarithmic with coverage. The Dubinin-Radushkevich isotherm assumes the multilayer character of adsorption and involves van der Waals forces (Hutson and Yang 1997).

The applicability of different isotherm equations was compared by evaluating the correlation coefficients  $R^2$  and chi-square ( $\chi^2$ ). The chi-square test measures difference in experimental and calculated data and its mathematical form is as follows:

$$\chi^2 = \sum \frac{(q_e \text{ exp} - q_e \text{ calc})^2}{q_e \text{ calc}}$$

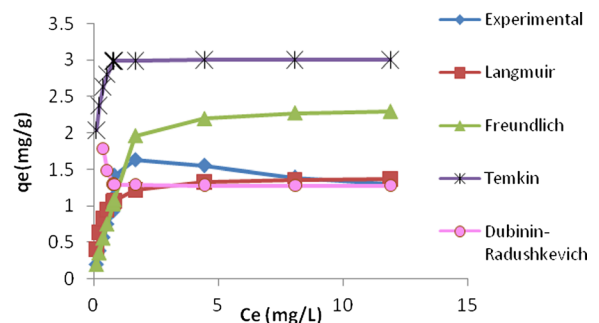


**Fig. 14** Comparative plots of isotherms with experimental data

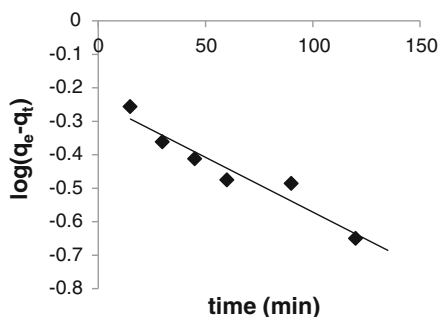


Fig. 15 Pseudo-first-order plot for Mg-HAP

If the  $\chi^2$  values are smaller, the model fits with the experimental data and vice versa.

Analyzing both  $R^2$  and  $\chi^2$  values, it was concluded that the Langmuir isotherm equation gave the most satisfactory fit with an adsorption capacity of 1.4 mg/g (25±2 °C) of Mg-HAP and a  $R_L$  value of 0.024 depicting favorable nature of the process. The  $K_{ap}$  value was found to be 5.472 which show high affinity of Mg-HAP adsorbent towards fluoride ions. The fit of the data to Langmuir isotherm model indicates that adsorption is monolayer in nature. Further, the experimental fluoride uptake capacity and the capacity predicted by different isotherms models were compared, and the results are presented in Fig. 14 which confirms Langmuir isotherm as the best model to describe the adsorption mechanism.

### 5 Kinetics of Fluoride Adsorption by Mg-HAP

In adsorption process, the rate of reaction is of prime importance and one of the most important factors that decides the design of adsorption equipment. For interpretation of the experimental data accurately, it is necessary to determine the steps in adsorption process which governs the overall rate of sorption. The rate-limiting step is also of great importance from the application point of view. The kinetics of adsorption was studied to explain the fluoride uptake mechanism in

Mg-HAP. It was observed that the uptake of fluoride increases with time. However, the adsorption of fluoride was rapid in the first 180 min after which the rate slowed down as the equilibrium approached.

The experimental adsorption data was analyzed by application of the pseudo-first-order and pseudo-second-order kinetic models. The linearized form of pseudo-first-order rate equation (Lagergren 1898) is given as follows:

$$\log(q_e - q_t) = \log q_e - \frac{b_1 t}{2.303}$$

The rate constant ( $b_1$ ) and theoretical equilibrium sorption capacities,  $q_e$ , calculated from the slope and intercept of the linear plots (Fig. 15) of the pseudo-first-order kinetic model, are given in Table 3.

The experimental data was also applied to the pseudo-second-order kinetic model (Ho 2006) given as follows:

$$\frac{t}{q_t} = \frac{1}{b_2 q_e^2} + \frac{t}{q_e}$$

The fit of this model is governed by a linear plot of  $t/q_t$  versus  $t$  as given in Fig. 16. The constants calculated from the slope and intercept of the plots are given in Table 3.

In order to test the contribution of intraparticle diffusion on the adsorption process, the rate constant for intraparticle diffusion was obtained by using the following equation (Wu et al. 2009):

$$q_t = k_i t^{1/2}$$

$q_t$  is plotted as a function of square root of time  $t^{1/2}$  as shown in Fig. 17. The  $k_i$  value was obtained from the slope of the linear portion of the curve. It was found that the plot is not entirely linear, but the graph reflects a two-staged nature. It is evident from the plots that there are two separate stages: first linear portion and second curved path followed by a plateau. This implies that a

Table 3 Values of adsorption rate constant for pseudo-first-order and pseudo-second-order kinetic models

Pseudo-first-order model parameters	Values	Pseudo-second-order model parameters	Values	Intraparticle diffusion model parameters	Values
$R^2$	0.927	$R^2$	0.997	$R^2$	0.951
$q_e$ (mg/g)	0.570	$q_e$ (mg/g)	0.980	$k_i$ (mg/g h <sup>1/2</sup> )	0.039
$b_1$ (min <sup>-1</sup> )	0.006	$b_2$ (g mg <sup>-1</sup> min <sup>-1</sup> )	0.031		
SSE	0.155	SSE	1.6E-3	SSE	0.18

SSE sum of errors squared

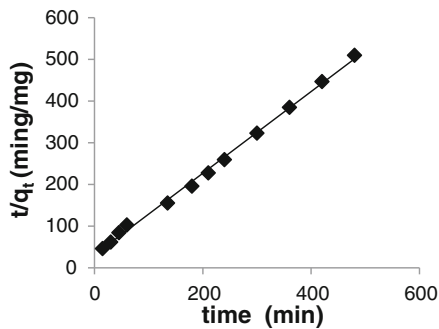


**Fig. 16** Pseudo-second-order plot for Mg-HAP

stage of intraparticle diffusion was continued up to 135 min followed by an equilibrium adsorption which began after 180 min. In other words, first stage is attributed to the immediate utilization of the most readily available adsorbing sites on the adsorbent surfaces. In second stage, very slow diffusion of adsorbate from surface site into the inner pores is observed. A similar behavior of the intraparticle diffusion curve with an initial linear portion and then a plateau was reported by researchers who worked on  $\text{KMnO}_4$ -modified activated carbon derived from steam pyrolysis of rice straw (Daifullah et al. 2007).

The kinetic models employed for fitting the adsorption data were assessed by calculating the sum of errors squared (SSE) which can be represented as written below:

$$\text{SSE} = \sum \frac{(q_{t \text{ exp}} - q_{t \text{ cal}})^2}{q_{t \text{ exp}}^2}$$

A lower value of SSE is considered to be a better fit to adsorption data (Ho 2004). The SSE values of the

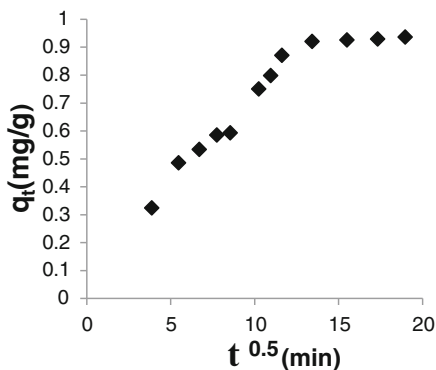


**Fig. 17** Intraparticle diffusion modeling of fluoride adsorption on Mg-HAP (dose 10 g/L,  $\text{F}^-$  concentration 10 mg/L, initial pH  $7.5 \pm 0.10$ ,  $T = 25 \pm 2$  °C)

kinetic models are summarized in Table 3. The values of  $R^2$  and SSE suggest that the sorption of fluoride by Mg-HAP follows a second-order reaction kinetic model and is also governed by intraparticle diffusion model.

## 6 Comparison with Other Adsorbents Used

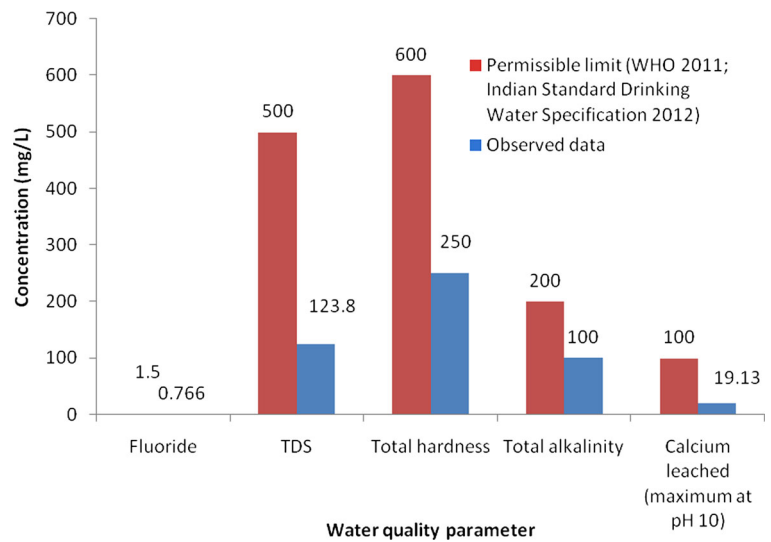
A comparison has been shown between Mg-HAP and adsorbents developed by some researchers with respect to their fluoride removal capacity (Table 4). Mg-HAP as a defluorinating agent has been found better than many adsorbents reported.

## 7 Water Quality Analysis

The treated water was tested for some key water quality parameters such as residual fluoride, calcium leached, TDS, total hardness, and alkalinity, which is detailed in Fig. 18. Electrical conductivity of the solution was  $246 \mu\text{s}/\text{cm}$ , and no turbidity was seen in the solution. To find out leaching of phosphorus from Mg-HAP, phosphorus content of the solution was evaluated to be  $0.67 \text{ mg}/\text{L}$  which was negligible. The residual fluoride

**Table 4** Comparative fluoride removal capacity of some adsorbents

Adsorbent	Reference	Removal capacity (mg/g)
Manganese dioxide-coated activated alumina	Tripathy and Raichur (2008)	1.22
Modified immobilized activated alumina	Rafique et al. (2012)	0.76
Nano-sized synthetic hydroxyapatite	Gao et al. (2009)	0.489
Activated quartz	Fan et al. (2003)	1.16
Calcite	Fan et al. (2003)	0.39
Lignite	Pekar et al. (2009)	0.71
Kaolinite clay	Gogoi and Baruah (2008)	0.0450
Montmorillonite	Tor (2006)	0.263
Laterite	Sarkar et al. (2006)	0.85
Charcoal	Bhargava and Killedar (1992)	$7.88 \times 10^{-5}$
Chitin composite	Davila-Rodriguez et al. (2009)	0.29
Mg-HAP	Present study	1.40

**Fig. 18** Water quality parameters of treated water

concentration in treated water was 0.766 mg/L which is below the permissible limit for intake of fluoride and just as required ( $>0.5$  mg/L) to counteract dental caries. It was observed that the water quality satisfies the WHO as well as the Indian Standard Drinking Water specification, and the treated water is consumable (WHO 2011; Indian Standard Drinking water specification 2012).

## 8 Conclusion

The following conclusions are drawn from the present study:

- The Mg-HAP adsorbent developed for fluoride removal from aqueous solution has very good potential for defluoridation with a capacity of 1.4 mg/g.
- Fluoride removal of 92.34 % was achieved with 10 g/L, and equilibrium was reached in 180 min. It was observed that increasing the amount of adsorbent and contact time increases the percentage of removal initially; however, gradually, it attains equilibrium and becomes constant.
- The adsorption capacity of Mg-HAP is not affected by pH of the medium. Calcium leaching in the solution was only observed at alkaline pH (9 and 10). Other anions such as nitrate and chloride do not affect the process significantly; however, the presence of bicarbonate, sulfate, and phosphate ions lowers the defluoridation capacity.

- The mechanism of fluoride removal follows both adsorption and ion exchange mechanism. Adsorption pattern follows Langmuir isotherm the best and the rate of reaction follows pseudo-second-order kinetics and the sorption of fluoride ion on Mg-HAP occurs through intraparticle diffusion pattern. Diffusion plays a key role in the adsorption of fluoride ions onto Mg-HAP, as depicted in intraparticle diffusion model.
- Various parameters tested for evaluating quality of treated water suggest that it is drinkable. The understanding gained from the results can be further applied for designing of adsorption systems for defluoridation of water for both domestic and community-based applications.

**Acknowledgments** The authors are thankful to Materials Research Centre, Malaviya National Institute Jaipur for providing all the characterization facilities needed for this paper.

## References

- APHA. (1995). *Standard methods* (19th ed.). Washington, DC: American Public Health Association.
- Ayoob, S., & Gupta, A. K. (2006). Fluoride in drinking water: a review on the status and stress effects. *Critical Reviews in Environmental Science and Technology*, 36(6), 433–487.
- Bhargava, D. S., & Killedar, D. J. (1992). Fluoride adsorption on fishbone charcoal through a moving media adsorber. *Water Research*, 26(6), 781–788.

- Chen, Q. Z., Wong, C. T., Lu, W. W., Cheung, K. M. C., Leong, J. C. Y., & Luk, K. D. K. (2004). Strengthening mechanisms of bone bonding to crystalline hydroxyapatite in vivo. *Biomaterials*, 25(18), 4243–4254.
- Choubisa, S. L., Choubisa, L., & Choubisa, D. (2009). Osteo-dental fluorosis in relation to nutritional status, living habits, and occupation in rural tribal areas of Rajasthan, India. *Fluoride*, 42, 210.
- Daifullah, A. A. M., Yakout, S. M., & Elreefy, S. A. (2007). Adsorption of fluoride in aqueous solutions using KMnO<sub>4</sub>-modified activated carbon derived from steam pyrolysis of rice straw. *Journal of Hazardous Materials*, 147, 633–643.
- Davila-Rodriguez, J. L., Escobar-Barrios, V. A., Shirai, K., & Rangel-Mendez, J. R. (2009). Synthesis of a chitin-based biocomposite for water treatment: optimization for fluoride removal. *Journal of Fluorine Chemistry*, 130(8), 718–726.
- Essadki, A. H., Gourich, B., Vial, C., Delmas, H., & Bennajah, M. (2009). Defluoridation of drinking water by electrocoagulation/electroflotation in a stirred tank reactor with a comparative performance to an external-loop airlift reactor. *Journal of Hazardous Materials*, 168(2), 1325–1333.
- Fan, X., Parker, D. J., & Smith, M. D. (2003). Adsorption kinetics of fluoride on low cost materials. *Water Research*, 37, 4929–4937.
- Fawell, K., Bailey, J., Chilton, E., Dahi, L., Fewtrell, Y., Magara. (2006) Fluoride in drinking-water. World Health Organization.
- Gao, S., Sun, R., Wei, Z., Zhao, H., Li, H., & Hu, F. (2009). Size-dependent defluoridation properties of synthetic hydroxyapatite. *Journal of Fluorine Chemistry*, 130(6), 550–556.
- George, S., Pandit, P., & Gupta, A. B. (2010). Residual aluminium in water defluoridated using activated alumina adsorption—modeling and simulation studies. *Water Research*, 44(10), 3055–3064.
- Gogoi, P. K., & Baruah, R. (2008). Fluoride removal from water by adsorption on acid activated kaolinite clay. *Indian Journal of Chemical Technology*, 15(5), 500–503.
- Gogoi, S., Nath, S. K., Bordoloi, S., & Dutta, R. K. (2015). Fluoride removal from groundwater by limestone treatment in presence of phosphoric acid. *Journal of Environmental Management*, 152, 132–139.
- He, G. L., & Cao, S. R. (1996). Assessment of fluoride removal from drinking water by calcium phosphate systems. *Fluoride*, 29(4), 212–216.
- Ho, Y. S. (2004). Citation review of Lagergren kinetic rate equation on adsorption reactions. *Scientometrics*, 59(1), 171–177.
- Ho, Y. S. (2006). Review of second-order models for adsorption systems. *Journal of Hazardous Materials*, 136(3), 681–689.
- Hu, K., & Dickson, J. M. (2006). Nanofiltration membrane performance on fluoride removal from water. *Journal of Membrane Science*, 279(1), 529–538.
- Hutson, N. D., & Yang, R. T. (1997). Theoretical basis for the Dubinin-Radushkevitch (DR) adsorption isotherm equation. *Adsorption*, 3(3), 189–195.
- Indian Standard Drinking Water Specification. (2012). Bureau of Indian Standards. IS 10500.
- Jain, S., & Jayaram, R. V. (2009). Removal of fluoride from contaminated drinking water using unmodified and aluminium hydroxide impregnated blue lime stone waste. *Separation Science and Technology*, 44(6), 1436–1451.
- Jimenez-Reyes, M., & Solache-Rios, M. (2010). Sorption behavior of fluoride ions from aqueous solutions by hydroxyapatite. *Journal of Hazardous Materials*, 180(1), 297–302.
- Lagergren, S. (1898). About the theory of so-called adsorption of soluble substances. *Kungliga Svenska Vetenskapsakademiens Handlingar*, 24, 1–39.
- Liu, H., Deng, S., Li, Z., Yu, G., & Huang, J. (2010). Preparation of Al–Ce hybrid adsorbent and its application for defluoridation of drinking water. *Journal of Hazardous Materials*, 179(1), 424–430.
- Long, H., Jin, Y., Lin, M., Sun, Y., Zhang, L., & Clinch, C. (2009). Fluoride toxicity in the male reproductive system. *Fluoride*, 42, 260–276.
- Maheshwari, R. C. (2006). Fluoride in drinking water and its removal. *Journal of Hazardous Materials*, 137(1), 456–463.
- Maliyekkal, S. M., Shukla, S., Philip, L., & Nambi, I. M. (2008). Enhanced fluoride removal from drinking water by magnesia-amended activated alumina granules. *Chemical Engineering Journal*, 140(1), 183–192.
- Mehta, D., George, S., & Mondal, P. (2014). Synthesis of hydroxyapatite by chemical precipitation technique and study of its biodegradability. *International Journal of Research in Advent Technology*, 2(4), 159–161.
- Mondal, P., & George, S. (2014). A review on adsorbents used for defluoridation of drinking water. *Reviews in Environmental Science and Biotechnology*, 14(2), 195–210.
- Mondal, P., George, S., & Mehta, D. (2014). Use of calcite for defluoridation of drinking water in acidic medium. *Research Journal of Chemical Science*, 4, 62–65.
- Murray, J. J. (Ed.). (1986). *Appropriate use of fluorides for human health*. Geneva: World Health Organization.
- Orlovskii, V. P., Komlev, V. S., & Barinov, S. M. (2002). Hydroxyapatite and hydroxyapatite-based ceramics. *Inorganic Materials*, 38(10), 973–984.
- Pekar, M. (2009). Fluoride anion binding by natural lignite (South Moravian Deposit of Vienna Basin). *Water Air Soil Pollution*, 197(1–4), 303–312.
- Percival, M. (1999). Bone health & osteoporosis. *Applied Nutritional Science Reports*, 5, 1–5.
- Rafique, A., Awan, M. A., Wasti, A., Qazi, I. A., & Arshad, M. (2012). Removal of fluoride from drinking water using modified immobilized activated alumina. *Journal of Chemistry*. doi:10.1155/2013/386476.
- Ramanan, S. R., & Venkatesh, R. (2004). A study of hydroxyapatite fibers prepared via sol–gel route. *Materials Letters*, 58(26), 3320–3323.
- Ravindra, K., & Garg, V. K. (2007). Hydro-chemical survey of groundwater of Hisar city and assessment of defluoridation methods used in India. *Environmental Monitoring and Assessment*, 132(1–3), 33–43.
- Russell, S. W., Luptak, K. A., Suchicital, C. T. A., Alford, T. L., & Pizziconi, V. B. (1996). Chemical and structural evolution of sol-gel-derived hydroxyapatite thin films under rapid thermal processing. *Journal of the American Ceramic Society*, 79(4), 837–842.
- Sakhare, N., Lunge, S., Rayalu, S., Bakardjiva, S., Subrt, J., Devotta, S., & Labhsetwar, N. (2012). Defluoridation of water using calcium aluminate material. *Chemical Engineering Journal*, 203, 406–414.
- Sargin, Y., Kizilyalli, M., Telli, C., & Güler, H. (1997). A new method for the solid-state synthesis of tetracalcium

- phosphate, a dental cement: X-ray powder diffraction and IR studies. *Journal of the European Ceramic Society*, 17(7), 963–970.
- Sarkar, M., Banerjee, A., Pramanick, P. P., & Sarkar, A. R. (2006). Use of laterite for the removal of fluoride from contaminated drinking water. *Journal of Colloid and Interface Science*, 302(2), 432–441.
- Sehn, P. (2007). Fluoride removal with extra low energy reverse osmosis membranes: three years of large scale field experience in Finland. *Desalination*, 223, 73–84.
- Sharma, J. D., Sohu, D., & Jain, P. (2009). Prevalence of neurological manifestations in a human population exposed to fluoride in drinking water. *Fluoride*, 42, 127–132.
- Spittle, B. (2008). Dyspepsia associated with fluoridated water. *Fluoride*, 41, 89.
- Sundaram, C. S., Viswanathan, N., & Meenakshi, S. (2008). Defluoridation chemistry of synthetic hydroxyapatite at nano scale: equilibrium and kinetic studies. *Journal of Hazardous Materials*, 155(1), 206–215.
- Sundaram, C. S., Viswanathan, N., & Meenakshi, S. (2009). Fluoride sorption by nano-hydroxyapatite/chitin composite. *Journal of Hazardous Materials*, 172(1), 147–151.
- Tatawat, R. K., & Chandel, C. S. (2008). A hydrochemical profile for assessing the groundwater quality of Jaipur City. *Environmental Monitoring and Assessment*, 143(1-3), 337–343.
- Tor, A. (2006). Removal of fluoride from an aqueous solution by using montmorillonite. *Desalination*, 201(1), 267–276.
- Tripathy, S. S., & Raichur, A. M. (2008). Abatement of fluoride from water using manganese dioxide-coated activated alumina. *Journal of Hazardous Materials*, 153(3), 1043–1051.
- Trivedi, M. H., Sangai, N. P., Patel, R. S., Payak, M., & Vyas, S. (2012). Assessment of groundwater quality with special reference to fluoride and its impact on IQ of schoolchildren in six villages of the Mundra region, Kachchh, Gujarat, India. *Fluoride*, 45, 377–383.
- WHO. (2011). *Guidelines for drinking-water quality, recommendations* (4th ed.). Geneva: World Health Organization.
- Wu, F. C., Tseng, R. L., & Juang, R. S. (2009). Initial behavior of intraparticle diffusion model used in the description of adsorption kinetics. *Chemical Engineering Journal*, 153(1), 1–8.